Cell Metabolism
Short Article

DNA Methylation Analysis in Nonalcoholic Fatty Liver Disease Suggests Distinct Disease-Specific and Remodeling Signatures after Bariatric Surgery

Markus Ahrens,[1,12] Ole Ammerpohl,[2,12] Witigo von Schönfels,[1,12] Julia Kolarova,[2] Susanne Bens,[2] Timo Itzel,[7] Andreas Teufel,[7] Alexander Herrmann,[3] Mario Brosch,[3] Holger Hinrichsen,[8] Wiebke Erhart,[3] Jan Egberts,[1] Bence Sipos,[9] Stefan Schreiber,[3] Robert Häsler,[6] Felix Stickel,[10] Thomas Becker,[1] Michael Krawczak,[4] Christoph Röcken,[5] Reiner Siebert,[2] Clemens Schafmayer,[1,13] and Jochen Hampe[3,11,13,*]

[1]Department of General and Thoracic Surgery
[2]Institute of Human Genetics
[3]Department of Internal Medicine I
[4]Institute for Medical Statistics and Informatics
[5]Institute of Pathology
[6]Institute for Clinical Molecular Biology
Christian-Albrechts-University Kiel/University Hospital Schleswig-Holstein, 24015 Kiel, Germany
[7]Department of Internal Medicine I, University Hospital Regensburg, 93053 Regensburg, Germany
[8]Gastroenterology and Hepatology Center Kiel, 24105 Kiel, Germany
[9]Institute of Pathology, University Hospital Tübingen, 72074 Tübingen, Germany
[10]Department of Clinical Research - Hepatology, University of Berne, CH-3010 Berne, Switzerland
[11]Department of Medicine I, University Hospital Dresden, 01307 Dresden, Germany
[12]These authors contributed equally to this work
[13]Co-senior authors
*Correspondence: jochen.hampe@uniklinikum-dresden.de
http://dx.doi.org/10.1016/j.cmet.2013.07.004

SUMMARY

Nonalcoholic fatty liver disease (NAFLD) is the most common chronic liver disorder in industrialized countries. Liver samples from morbidly obese patients (n = 45) with all stages of NAFLD and controls (n = 18) were analyzed by array-based DNA methylation and mRNA expression profiling. NAFLD-specific expression and methylation differences were seen for nine genes coding for key enzymes in intermediate metabolism (including *PC*, *ACLY*, and *PLCG1*) and insulin/insulin-like signaling (including *IGF1*, *IGFBP2*, and *PRKCE*) and replicated by bisulfite pyrosequening (independent n = 39). Transcription factor binding sites at NAFLD-specific CpG sites were >1,000-fold enriched for ZNF274, PGC1A, and SREBP2. Intraindividual comparison of liver biopsies before and after bariatric surgery showed NAFLD-associated methylation changes to be partially reversible. Postbariatric and NAFLD-specific methylation signatures were clearly distinct both in gene ontology and transcription factor binding site analyses, with >400-fold enrichment of NRF1, HSF1, and ESRRA sites. Our findings provide an example of treatment-induced epigenetic organ remodeling in humans.

INTRODUCTION

Nonalcoholic fatty liver disease (NAFLD) describes a spectrum of liver disorders that occurs in the context of obesity and type 2 diabetes mellitus (Chalasani et al., 2012). While pure steatosis is a largely benign condition, it can be complicated by nonalcoholic steatohepatitis (NASH), which can progress to cirrhosis and liver failure. The pathogenesis of NAFLD is multifactorial and triggered by environmental factors such as hypercaloric nutrition and lack of physical activity in the context of genetic predisposition (Chalasani et al., 2010; Romeo et al., 2008). Bariatric surgery is the most radical therapy for the metabolic syndrome and NASH, leading typically to massive weight loss, improvement of liver histology (Dixon et al., 2004), and all-cause mortality (Lundell, 2012).

DNA methylation represents a level of epigenetic regulation that is closely linked to transcription factor (TF) binding and chromatin accessibility. While DNA methylation been studied intensively in cancer, including hepatocellular carcinoma (Ammerpohl et al., 2012), its pathogenetic role in benign disorders is only recently being recognized. DNA methylation signatures are not static but can be remodeled by TFs (Stadler et al., 2011) and by environmental stimuli (Barrès et al., 2012). The relevance of differential DNA methylation in NAFLD has been demonstrated for PPARGC1A, which showed a tight interaction to the insulin resistance phenotype (Sookoian et al., 2010) and by differential susceptibility of mice to hepatic steatosis (Pogribny et al., 2009) based on their epigenetic profiles.

Here we present a systematic analysis of DNA methylation in NAFLD and its dynamic remodeling after the massive weight loss induced by bariatric surgery.

RESULTS

Differences in DNA Methylation between Liver Phenotypes

Snap-frozen liver biopsies were obtained from 63 patients and classified histologically using the nonalcoholic fatty liver activity

Table 1. Sample Overview for the Discovery and Replication Samples

		Liver Phenotype Samples				Bariatric Samples		
		Normal Controls (C)	Healthy Obese (H)	Steatosis (S)	NASH (N)	Prebariatric (B1)	Postbariatric (B2)	Delta
Discovery	N methylation	18	18	12	15	n/a	23	n/a
	Age	51 [44–72]	44 [41–50]	46 [37–49]	47 [40–50]	47 [38–51]		n/a
	BMI	24 [21–26]	45 [42–49]	50 [47–55]	49 [44–56]	48 [45–54]	34 [30–40]	14 [12–16]
	Weight (kg)	67 [58–64]	135 [122–150]	147 [121–166]	146 [133–168]	146 [134–160]	106 [87–116]	−40 [−49– −34]
	Sex (% male)	50	0	42	27	17	17	n/a
	Diabetes (%)	11	17	25	20	26	17	−9
	Fat (area in %)	0 [0–1]	3 [0–4]	43 [20–70]	75 [70–85]	30 [12–70]	0 [3–25]	16 [5–40]
	Inflammation (0–3)	0 [0–0]	0 [0–0]	0 [0–0]	2 [1–2]	0 [0–1]	0 [0–0]	0 [1–0]
	Fibrosis (0–4)	0 [0–0]	0 [0–0]	0 [0–1]	1 [0–1]	0 [0–1]	0 [0–0]	0 [0–1]
	NAS (0–8)	0 [0–0]	0 [0–0]	2 [1–3]	5 [5–6]	2 [1–5]	0 [0–1.5]	2 [1–3]
	N mRNA (N overlap with methylation set)	12 (11)	16 (16)	9 (8)	17 (15)	n/a	16 (16)	n/a
Replication	N	10	9	10	10			
	Age	74 [66–77]	37 [34–43]	42 [31–59]	40 [35–47]			
	BMI	25 [23–26]	48 [46–51]	47 [40–57]	58 [57–59]			
	Weight (kg)	67 [62–72]	137 [128–144]	140 [117–162]	165 [159–186]			
	Sex (% male)	20	11	10	20			
	Diabetes (%)	20	0	40	20			
	Fat (area in %)	0 [0–0]	3 [2–5]	65 [31–78]	80 [70–82]			
	Inflammation (0–3)	0 [0–0]	0 [0–0]	0 [0–0]	1 [1–2]			
	Fibrosis (0–4)	0 [0–0]	0 [0–0]	0 [0–0]	1 [1–1]			
	NAS (0–8)	0 [0–0]	0 [0–1]	2 [1–3]	5 [5–6]			

The median and the interquartile range are provided for all numeric parameters. All prebariatric patients and no postbariatric patients are part of the liver phenotype samples. For the postbariatric samples, the change in the parameters is provided in the separate column. RNA for expression analysis was available for 70 liver samples, of which 66 were obtained from the same individuals who were used in the methylation experiment (in brackets). "Bariatric samples" refers strictly to patients for whom paired biopsies were available. The majority of the "liver phenotype samples" (H/S/N, 82%, 87%, and 90%) were obtained during bariatric surgery as well.

score (Kleiner et al., 2005) and clinically into normal controls (n = 18), healthy obese (n = 18), steatosis (n = 12), and NASH (n = 15). These biopsies are referred to as "liver phenotype samples." For 23 of these individuals (H/S/N: 7/10/6), follow-up liver biopsies 5–9 months after bariatric surgery were available. These postsurgery samples are referred to as "bariatric samples," bringing the total of analyzed liver biopsies to 86. The bariatric patients showed the expected improvement of liver histology (Dixon et al., 2004; Mathurin et al., 2006) (Table 1). All samples were assayed for CpG methylation at over 450,000 sites using an array-based approach. Array-based mRNA expression data were available for 70 liver samples, of which 66 were obtained from the same individuals as used in the methylation experiment (Table 1).

First, all sites deviating at least in one of the four phenotypic groups from the overall median methylation were identified using an omnibus (Kruskal-Wallis) test at a nominal significance of $p < 0.0001$. For the 273 CpG sites meeting this significance criterion, the medians of DNA methylation for each phenotype were sorted from lowest to highest. Under the null hypothesis, each of the 24 possible phenotype permutations would be equally abundant. However, particular ordered phenotype permutations were found to be strongly enriched ($p < 10^{-14}$, see Table S1A online), namely those compatible with a phenotypic progression from normal controls (C) to healthy obese (H), to steatosis (S), to NASH (N).

Second, we aimed to identify CpGs differentially methylated between phenotypic groups. In a global cluster and principal components analysis (PCA) at a false discovery threshold level of $q = 0.05$, 467 CpG loci were identified to be differentially methylated between the four phenotypic groups (online supplements can be found at http://gengastro.1med.uni-kiel.de/suppl/methyl_liver/). For ease of visualization, this analysis was repeated using $q = 0.004$, yielding 74 differentially methylated sites (Figure 1A). Both the heatmap and the PCA of these differentially methylated sites show normal liver samples and NASH as the extreme groups with healthy obese and steatosis samples located in the intermediate.

Expression Differences of Transcripts in the Liver Phenotype Comparison

Messenger RNA expression for the 294 genes annotated to the 467 CpGs differentially methylated between the four phenotypic groups was analyzed: 272 of these genes were present on the expression array. Analyses were restricted to CpG sites with at least a 5% difference of methylation between the phenotypic

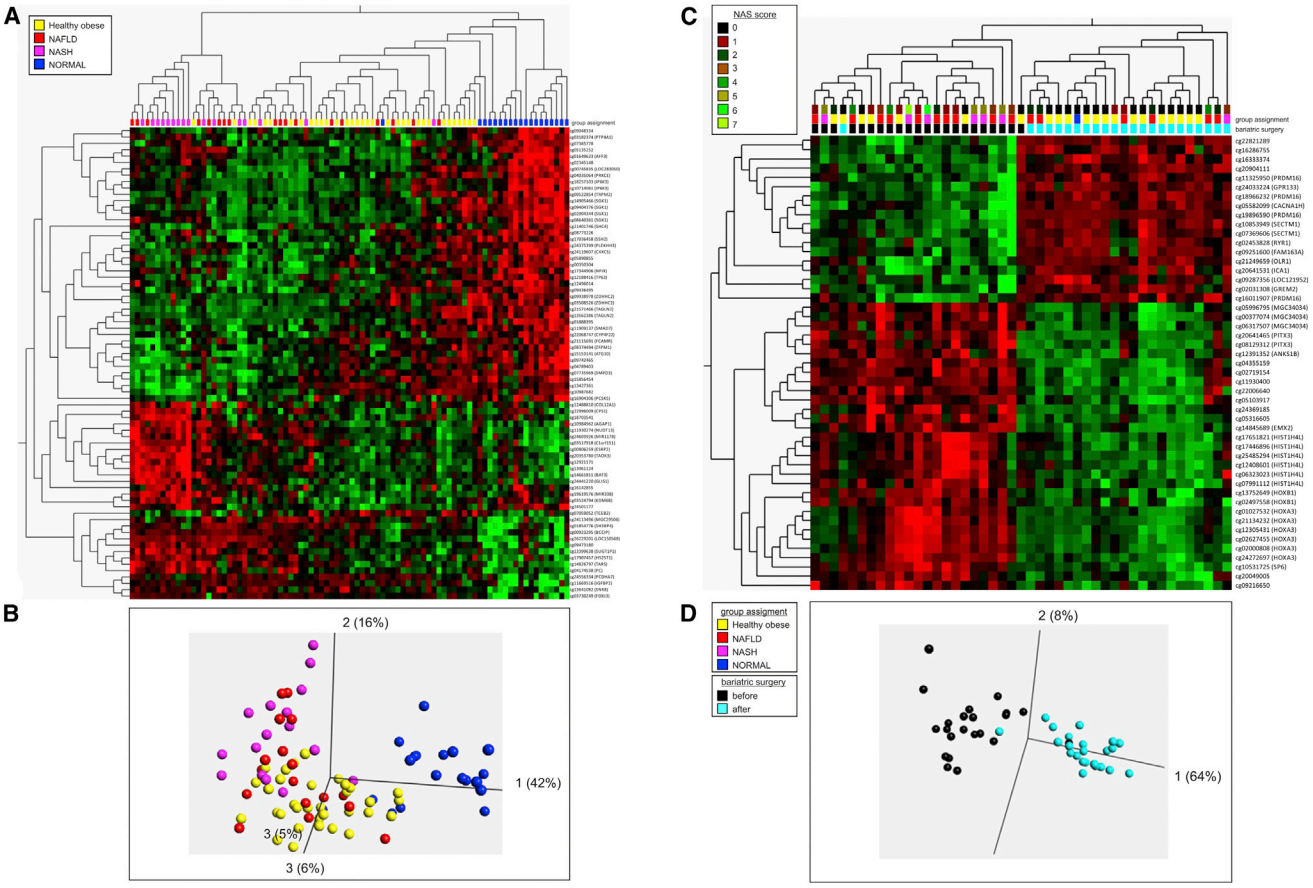

Figure 1. Global Analysis of Methylation in Phenotypic Groups and after Bariatric Surgery

(A and B) Global analysis of the methylation patterns of the phenotypic groups (normal controls, healthy obese, steatosis and NASH). (A) shows a heatmap of the 74 CpGs resulting from an ANOVA analysis using an FDR <0.004. If the CpG is assigned to a gene locus, the respective gene name is provided in brackets. For visualization, the means and variances are normalized to 0 and 1, respectively, for each gene. (B) shows the first three principal components analysis (PCA) of the corresponding PCA.

(C and D) Analysis of the alteration in methylation patterns before and after bariatric surgery. (C) shows a heatmap of the 49 CpGs resulting from an ANOVA analysis using an FDR < 0.01. If the CpG is assigned to a gene locus, the respective gene name is provided in brackets. (D) shows the first three PCA of the corresponding PCA. See also Figure S1.

extremes of normal controls and NASH and a minimum $\log_2$ change in mRNA expression of the respective gene/mRNA of 0.2. According to these criteria, nine of the differentially methylated genes also showed differential expression ($p < 0.05$ corrected for multiple testing, Online Supplement, http://gengastro.1med.uni-kiel.de/suppl/methyl_liver/). With the exception of *GRID1*, expression and methylation at these loci were closely inversely correlated, suggesting a causal role of DNA methylation for differential expression of these genes in the liver phenotypes (Figure S1A). Differential methylation for the nine putative driver genes was technically validated in 42 samples and replicated in 39 independent samples (C/H/S/N, 10/9/10/10) at a nominal significance level of $p < 0.05$ using bisulfite pyrosequencing as an independent technology (Figure S2, Table 2).

Postbariatric Changes in CpG Methylation

The potential reversibility of DNA methylation changes associated with the progression from normal controls to NASH was evaluated. This was possible, because the postbariatric samples were not used to determine the liver phenotype associated DNA methylation patterns. A significant—though weak—inverse correlation (Spearman rank test, $p = 0.004$, $\varrho = -0.13$) of DNA methylation changes between NASH and normal controls on the one hand and after (B2, i.e., "healthier," improved histology) and before (B1) bariatric surgery on the other hand was seen for the 467 CpG sites identified in the liver phenotype analysis. This effect seen more clearly in the analysis of loci identified in the pairwise comparison of CpG methylation between normal controls and NASH at the $q = 0.05$ level by OMICs explorer (list of CpGs not shown) yielding a p value of 1.6×10^{-7} ($\varrho = -0.23$). However, as reflected by the correlation coefficients of –0.13 and –0.23, disease-associated methylation was only partially reversible and restricted to a subset of loci. In a single CpG-based test of differential methylation corrected for multiple testing, phenotype-associated methylation at the *HOXB1*, *PRKCZ*, *SLC38A10*, and *SECTM1* loci was reversible (Online Supplement, http://gengastro.1med.uni-kiel.de/suppl/methyl_liver/).

Table 2. Candidate Epigenetic Disease Driver Genes

Gene	CpG Site	p_{GROUP}	P_{NC}	P_{REPLIC}	Δ_{EXPR_NC}	Δ_{Meth_NC}	Gene Name	putative function
GALNTL4	cg16337763	1.5×10^{-6}	1.5×10^{-05}	0.0017	0.70	−0.10	Putative polypeptide N-acetylgalactosaminyl-transferase-like protein 4	May catalize the initial reaction in O-linked oligosaccharide biosynthesis
ACLY	cg25687894	6.1×10^{-5}	5.4×10^{-03}	0.0036	0.38	−0.09	ATP citrate lyase	Primary enzyme for synthesis of cytosolic acetyl-CoA
GRID1	cg27317356	8.5×10^{-5}	1.1×10^{-04}	0.0026	1.35	0.13	Glutamate receptor delta-1	Synaptic activity, expressed in liver, function in relation to liver metabolism poorly studied
IGFBP2	cg11669516	3.6×10^{-4}	2.4×10^{-04}	0.015	−1.43	0.20	Insulin-like growth factor binding protein 2	Leptin-regulated; overexpression reversed diabetes in murine models
PLCG1	cg18347630	2.5×10^{-4}	3.6×10^{-03}	0.0031	0.33	−0.05	Phospholipase C-gamma-1	Production of diacylglycerol and inositol 1,4,5-trisphosphate (IP3)
PRKCE	cg04035064	2.8×10^{-4}	2.7×10^{-03}	0.0035	0.85	−0.12	Protein kinase C, epsilon	Phospholipid- and diacylglycerol-dependent serine/threonine-protein kinase with broad regulatory functions
IGF1	cg08806558	1.8×10^{-3}	2.8×10^{-04}	0.013	−0.93	0.13	Insulin-like growth factor 1	Hormone similar in structure to insulin, promotes growth, regulates glucose uptake, glycogen synthesis, cell proliferation
IP6K3	cg10714061	3.4×10^{-4}	3.4×10^{-04}	0.037	1.04	−0.21	Inositol hexaphosphate kinase 3	Converts inositol hexakisphosphate (InsP6) to diphosphoinositol pentakisphosphate (InsP7/PP-InsP5)
PC	cg04174538	4.0×10^{-3}	3.4×10^{-04}	0.0027	−0.48	0.07	Pyruvate carboxylase	initial reaction of glucose and lipid synthesis from pyruvate

Genes with CpG sites differentially methylated between phenotypic groups with concomitant significant mRNA expression differences (normalized $\log_2$ values). The data are a subset filtered from the online supplement according to the criteria provided in the Results. P_{GROUP} denotes the p value of the global phenotype association, P_{NC} the pairwise comparison of the N and C group, and P_{REPLIC} the independent replication p value in the methylation analysis. Δ_{EXPR_NC} refers to the log2 expression difference between the N and C groups and Δ_{Meth_NC} to the respective absolute difference in methylation. Positive values in these two columns refer to higher values in the C group as compared to N (as calculated by N minus C). See also Figures S1 and S2.

In a paired analysis of CpG methylation before and after bariatric surgery, a clear separation in the principal components analyses according to the bariatric surgery status was seen (Figure 1C). A total of 113 differentially methylated sites were identified (q = 0.05). For these sites, a strong correlation of differential methylation between the liver phenotypes (C versus N) and bariatric surgery was observed ($p < 2.2 \times 10^{-16}$, ϱ = –0.94); i.e., those CpGs losing methylation after bariatric surgery typically gained methylation during progression from normal liver to NASH and vice versa. Only four CpGs (two unannotated and two in the *HOXB1* locus) overlapped with the sites identified in the phenotype group analyses at the same false discovery rate (q = 0.05). Of the 113 CpGs from the bariatric analysis, 80 mapped to 32 gene loci, of which the gene encoding protein-tyrosine phosphatase epsilon (*PTPE*) showed both differential expression before and after bariatric surgery (last panel, Figure 2).

Gene Ontology Analysis

The ten highest ranking gene ontology (GO) analysis terms from the liver phenotype and bariatric analyses were compared. Only four of the top ten terms were identical and included generic biological processes. Interestingly, the six GO terms specific for the bariatric analysis revealed terms sharing remodeling and anatomical structure development as a common theme and included "anatomical structure development" and "anatomical structure morphogenesis" (Table S2B).

Enrichment of Transcription Factor Binding Sites

We investigated whether the CpG sites differentially methylated between liver phenotypes or after bariatric surgery were enriched for binding sites of any of the 73 TFs annotated in the liver cell line HepG2 cells in the recently published ENCODE data set (Dunham et al., 2012; Gerstein et al., 2012; Neph et al., 2012).

Highly significant enrichment of TF binding sites in both the phenotype and bariatric remodeling groups was seen for TFs ZNF274 (zinc finger protein 274, >7,000-fold enrichment in both groups, maximum p value $p < 1.0 \times 10^{-300}$, Fisher's exact test), PGC1A (peroxisome proliferator-activated receptor gamma, coactivator 1 alpha, >2,000-fold, $p < 1.0 \times 10^{-300}$), SREBP2 (sterol regulatory element binding TF 2, >1,000-fold, $p < 3.8 \times 10^{-272}$), and GRP20 (glycine-rich protein 20, >400-fold, $p < 3.8 \times 10^{-233}$), implicating an involvement of these factors in both disease and remodeling. While only eight TFs, namely ZNF274, PGC1A, SREBF2, GRP20, ZEB1, FOXA1, FOXA2, and RXA, were enriched in the phenotype group using a cutoff of $p < 0.007$ ($p < 0.05$ corrected for 73 tests), binding sites from 38 TFs were significantly enriched in the

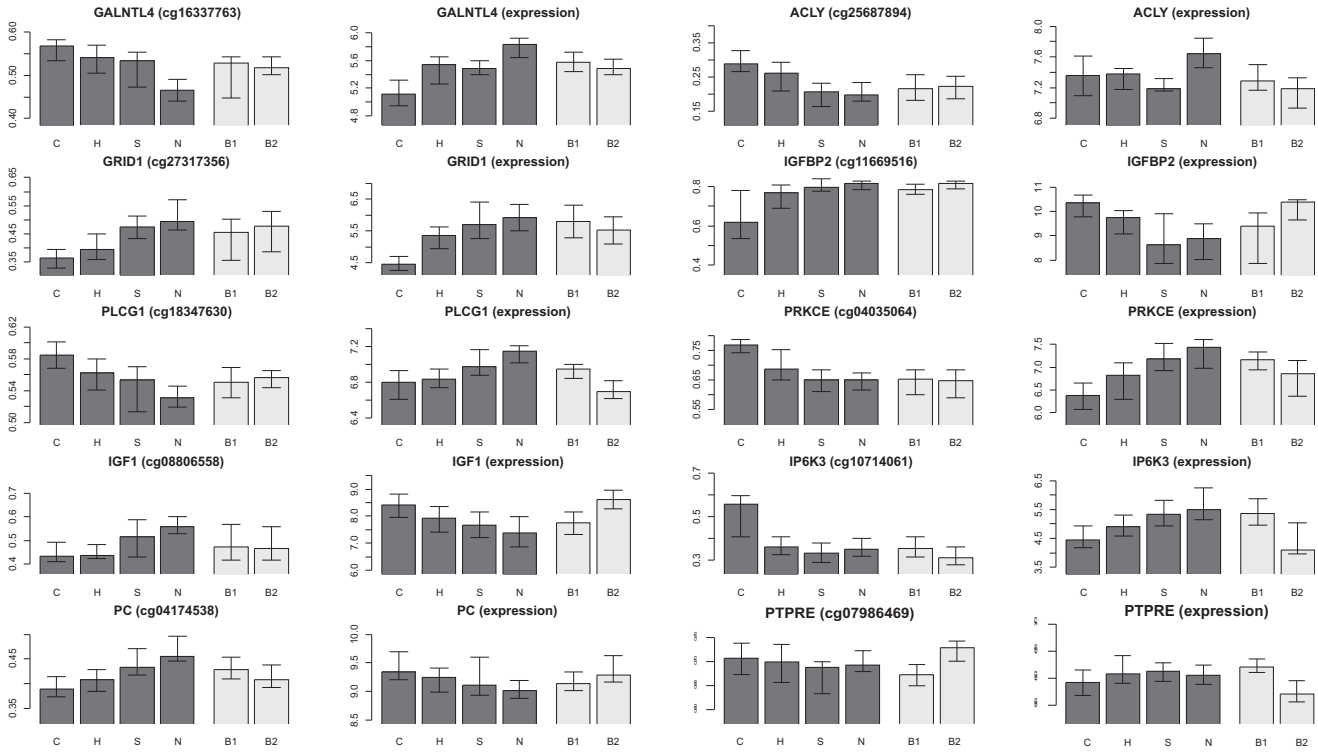

Figure 2. Methylation and Expression Data of Candidate Epigenetic Disease Driver Genes

Detailed depiction of the nine loci from the phenotype group analysis which showed both significant differences in methylation and mRNA expression in the liver phenotype analysis. For each gene, the methylation data are given on the left side and the expression data on the right side. Groups are denoted as C (normal controls), H (healthy obese), S (steatosis), N (NASH), B1 (before bariatric surgery), and B2 (after bariatric surgery). The tenth panel (bottom right) displays *PTPE*, the one gene with significant changes both in the bariatric expression and methylation analysis. Error bars represent the interquartile ranges as calculated by boxplot.stats() in R. See also Figure S2.

bariatric CpG methylation signature, pointing to a broad reprogramming of the liver cells during this process. TFs with the highest relative enrichment in the bariatric as compared to the liver phenotype analysis included NRF1 (nuclear respiratory factor 1, 466-fold), HSF1 (heat shock TF 1, 463-fold), ESRRA (estrogen-related receptor alpha, 454-fold), SRF (serum response factor, 232-fold), TR4 (testicular receptor 4, 232-fold), CEBPZ (CCAAT/enhancer binding protein zeta, 231-fold), and SREBP1 (sterol regulatory element binding TF, 153-fold). A full list for all TF binding sites including mRNA expression analysis in both the phenotypic and bariatric comparisons is provided in Table S2.

DISCUSSION

Methylation as a Molecular Clock in the Model of Disease Progression

CpG methylation may be used a "molecular clock" during the development of the liver phenotype, which is thought to progress from normal liver histology (i.e., "healthy obese" individuals [Blüher, 2010; Kusminski et al., 2012; Tran et al., 2008]) through simple steatosis to steatotic necroinflammation. Indeed, differentially methylated CpG sites in the liver phenotype analysis with either progressively increasing or decreasing methylation across this phenotypic axis were highly overrepresented.

Candidate Epigenetic Regulators of Disease

Nine genes showing both differential methylation and mRNA expression were identified. The absolute differences in CpG methylation between groups typically ranged between 5% and 15% and may reflect subpopulations of hepatocytes. Although only a fraction of those has been studied in detail in relation to NAFLD, their known functions are compatible with a putative role as key drivers of the liver phenotype. They include key enzymes catalyzing the initial steps in glucose, lipid, acetyl-CoA, and oligosaccharide synthesis and pathway members of insulin-like signaling mediators. A true mechanistic understanding and experimental proof of this disease driver claim will require further experiments. For two (ACLY, IGFBP2) of the nine putative driver genes, high-quality mechanistic studies in NASH models are available: ACLY (ATP citrate lyase) catalyzes conversion of citrate into acetyl-CoA, the building block for the endogenous biosynthesis of fatty acids (Chypre et al., 2012), putting this enzyme at a crosslink between glucose metabolism and fatty acid synthesis. Its mRNA is regulated by SREBP-1, one of the TFs implicated in the bariatric remodeling response in this study (Bauer et al., 2005). Abrogation of hepatic ACLY, which is upregulated in our human mRNA data set, protects against steatosis in leptin-receptor-deficient mice (Wang et al., 2009). The *IGFBP2* (insulin-like growth factor binding protein 2) locus was hypermethylated and its mRNA downregulated in NASH.

This observation is consistent with animal data, as adenoviral overexpression of IGFBP2 has been shown to reverse diabetes and steatosis in obese mice (Hedbacker et al., 2010).

A key role for IGF1 (insulin-like growth factor 1), a hormone responsible for many of the systemic effects of growth hormone (GH), for liver metabolism is increasingly being recognized (Takahashi, 2012). Low serum IGF1 (consistent with the liver data obtained in this study) has been identified as a marker of liver steatosis and NASH (García-Galiano et al., 2007). Mice with a liver-specific deletion of the growth hormone receptor, which show a >90% reduction of IGF-1, exhibited severe hepatic steatosis (Fan et al., 2009).

This study did not include patients with advanced NASH and high fibrosis grades. While this provides a relatively homogenous phenotype spectrum and ensures a more homogenous cell population between phenotype groups, it limits the applicability of our findings. Indeed, fibrosis progression will likely have a distinct epigenetic signature that is not reflected in our results.

Remodeling Signature after Weight Loss

Both GO and TF binding site analysis revealed striking differences between the liver phenotype and bariatric comparisons.

An inverse correlation of NASH phenotype and bariatric remodeling was observed, indicating that NASH-associated methylation changes can indeed be reversed. The gene encoding protein-tyrosine phosphatase epsilon (*PTPRE*) showed both a differential expression and differential methylation before and after bariatric surgery. Hypermethylation and transcriptional downregulation of PTPRE—which is a negative regulator of insulin signaling in skeletal muscle (Aga-Mizrachi et al., 2008)—after bariatric surgery may thus represent a key mechanism in the restitution of hepatic insulin sensitivity during weight loss.

While the presented study is limited in terms of sample size, phenotype coverage, and technology, it represents a genome-wide assessment of CpG methylation in NAFLD and its dynamic change induced by the weight loss after bariatric surgery in humans. Some of the candidate epigenetic driver genes may represent attractive targets for future mechanistic studies and therapeutic interventions. Likewise, the epigenetic remodeling signature after bariatric surgery provides a data set of epigenetic organ remodeling in humans and may add to our understanding of liver regeneration.

EXPERIMENTAL PROCEDURES

Patient Samples

Liver samples were obtained percutaneously for patients undergoing liver biopsy for suspected NAFLD or intraoperatively for assessment of liver histology. Normal control samples were recruited from samples obtained for exclusion of liver malignancy during major oncological surgery. None of the normal control individuals underwent preoperative chemotherapy, and liver histology demonstrated absence of both cirrhosis and malignancy. Consenting patients underwent a routine liver biopsy during bariatric surgery for assessment of liver affection. Biopsies were immediately frozen in liquid nitrogen, ensuring an ex vivo time of less than 40 s in all cases. A percutaneous follow-up biopsy was obtained in consenting bariatric patients 5–9 months after surgery. Patients with evidence of viral hepatitis, hemochromatosis, or alcohol consumption greater than 20 g/day for women and 30 g/day for men were excluded. All patients provided written, informed consent. The study protocol was approved by the institutional review board ("Ethikkommission der Medizinischen Fakultät der Universität Kiel," D425/07, A111/99) before the commencement of the study. Standardized histopathological assessment (Kleiner et al., 2005) was performed by a single pathologist blinded to the molecular analyses. Of the 23 postbariatric patients, 20 underwent a sleeve gastrectomy and 3 a gastric bypass procedure.

DNA Methylation and Expression Analysis

For homogenization of 5–10 mg frozen tissue and subsequent nucleic acid isolation, tubes with 1,4 mm ceramic beads (Precellys, Villeurbanne, France) and the AllPrep DNA/RNA Mini Kit (QIAGEN, Hilden, Germany) were used. Bisulfite conversion used the Zymo EZ DNA Methylation Kit (Zymo Research, Orange, CA, USA). Hybridization of the HumanMethylation450k Bead Chip (Illumina, SanDiego, CA), subsequent scanning (iScan, Illumina), and mRNA expression analysis using the HuGene 1.1 ST gene (Affymetrix, Santa Clara, Ca, USA) were performed according to the manufacturers protocols. DNA and RNA chip data are available in GEO (GSE48325, GSE48452).

Statistics and Data Analysis

Hybridization signals were analyzed using GenomeStudio software (default settings; GenomeStudio version 2011.1, Methylation Analysis Module version 1.9.0; Illumina Inc) and internal controls for normalization. Identification of differentially methylated loci and generation of the heat maps or pairwise group comparisons analysis followed by cluster analyses, and PCA was performed using the OMICS explorer (version 2.3, Qlucore, Lund, Sweden). If not otherwise stated, clustering was based on correlation (mean = 0, variance = 1). The weighted average was used to generate the heatmaps.

All other analyses were performed in R (R Development Core Team, 2010). Pairwise comparisons of methylation or mRNA expression differences were performed using the Wilcoxon test.

Gene Ontology Analysis

GO analyses for biological process were performed using topGO package (Alexa et al., 2006) in R. The minimal nominal uncorrected p value of each gene from the Wilcoxson test in the pairwise group comparisons was used as a weight vector in the "classic" Komolgorov-Smirnov test as implemented in the topGO package. GO analyses was restricted to terms with a node size of $\geq$10. Only CpG sites that were annotated to a gene locus (Illumina) were utilized.

Analysis of Transcription Factor Binding Enrichment

For enrichment analysis of CpG islands in liver-specific open chromatin structures, the called peaks of signal enrichment based on pooled, normalized (interpreted) data for the HepG2 cell line were downloaded on 10/16/2012 from the ENCODE Open Chromatin by DNaseI HS Track (http://genome.ucsc.edu/cgi-bin/hgTrackUi?g=wgEncodeDNAseSuper). The called peaks for signal enrichment of TF binding sites in the HepG2 cell line were downloaded from the ENCODE Transcription Factor Binding Track on September 15, 2012. CpGs that mapped within or ±1 bp of an annotated TF binding site were considered positive for the respective TF.

SUPPLEMENTAL INFORMATION

Supplemental Information includes two figures, two tables, and Supplemental Experimental Procedures and can be found with this article online.

ACKNOWLEDGMENTS

This study was supported by the German Ministry of Education and Research (BMBF) through the Virtual Liver Project and through institutional funds from the Medical Faculty of the University of Kiel.

Received: December 6, 2012
Revised: May 12, 2013
Accepted: July 12, 2013
Published: August 6, 2013

REFERENCES

Aga-Mizrachi, S., Brutman-Barazani, T., Jacob, A.I., Bak, A., Elson, A., and Sampson, S.R. (2008). Cytosolic protein tyrosine phosphatase-epsilon is a negative regulator of insulin signaling in skeletal muscle. Endocrinology *149*, 605–614.

Alexa, A., Rahnenführer, J., and Lengauer, T. (2006). Improved scoring of functional groups from gene expression data by decorrelating GO graph structure. Bioinformatics *22*, 1600–1607.

Ammerpohl, O., Pratschke, J., Schafmayer, C., Haake, A., Faber, W., Von Kampen, O., Brosch, M., Sipos, B., Von Schönfels, W., Balschun, K., et al. (2012). Distinct DNA methylation patterns in cirrhotic liver and hepatocellular carcinoma. International Journal of Cancer. Journal International Du Cancer *130*, 1319–1328.

Barrès, R., Yan, J., Egan, B., Treebak, J.T., Rasmussen, M., Fritz, T., Caidahl, K., Krook, A., O'Gorman, D.J., and Zierath, J.R. (2012). Acute exercise remodels promoter methylation in human skeletal muscle. Cell Metab. *15*, 405–411.

Bauer, D.E., Hatzivassiliou, G., Zhao, F., Andreadis, C., and Thompson, C.B. (2005). ATP citrate lyase is an important component of cell growth and transformation. Oncogene *24*, 6314–6322.

Blüher, M. (2010). The distinction of metabolically 'healthy' from 'unhealthy' obese individuals. Curr. Opin. Lipidol. *21*, 38–43.

Chalasani, N., Guo, X., Loomba, R., Goodarzi, M.O., Haritunians, T., Kwon, S., Cui, J., Taylor, K.D., Wilson, L., Cummings, O.W., et al. (2010). Genome-wide association study identifies variants associated with histologic features of nonalcoholic fatty liver disease. Gastroenterology *139*, 1567–1576, 1576.e1–1576.e6.

Chalasani, N., Younossi, Z., Lavine, J.E., Diehl, A.M., Brunt, E.M., Cusi, K., Charlton, M., and Sanyal, A.J.; American Gastroenterological Association; American Association for the Study of Liver Diseases; American College of Gastroenterologyh. (2012). The diagnosis and management of non-alcoholic fatty liver disease: practice guideline by the American Gastroenterological Association, American Association for the Study of Liver Diseases, and American College of Gastroenterology. Gastroenterology *142*, 1592–1609.

Chypre, M., Zaidi, N., and Smans, K. (2012). ATP-citrate lyase: a mini-review. Biochem. Biophys. Res. Commun. *422*, 1–4.

Dixon, J.B., Bhathal, P.S., Hughes, N.R., and O'Brien, P.E. (2004). Nonalcoholic fatty liver disease: improvement in liver histological analysis with weight loss. Hepatology *39*, 1647–1654.

Dunham, I., Kundaje, A., Aldred, S.F., Collins, P.J., Davis, C.A., Doyle, F., Epstein, C.B., Frietze, S., Harrow, J., Kaul, R., et al.; ENCODE Project Consortium. (2012). An integrated encyclopedia of DNA elements in the human genome. Nature *489*, 57–74.

Fan, Y., Menon, R.K., Cohen, P., Hwang, D., Clemens, T., DiGirolamo, D.J., Kopchick, J.J., Le Roith, D., Trucco, M., and Sperling, M.A. (2009). Liver-specific deletion of the growth hormone receptor reveals essential role of growth hormone signaling in hepatic lipid metabolism. J. Biol. Chem. *284*, 19937–19944.

García-Galiano, D., Sánchez-Garrido, M.A., Espejo, I., Montero, J.L., Costán, G., Marchal, T., Membrives, A., Gallardo-Valverde, J.M., Muñoz-Castañeda, J.R., Arévalo, E., et al. (2007). IL-6 and IGF-1 are independent prognostic factors of liver steatosis and non-alcoholic steatohepatitis in morbidly obese patients. Obes. Surg. *17*, 493–503.

Gerstein, M.B., Kundaje, A., Hariharan, M., Landt, S.G., Yan, K.-K., Cheng, C., Mu, X.J., Khurana, E., Rozowsky, J., Alexander, R., et al. (2012). Architecture of the human regulatory network derived from ENCODE data. Nature *489*, 91–100.

Hedbacker, K., Birsoy, K., Wysocki, R.W., Asilmaz, E., Ahima, R.S., Farooqi, I.S., and Friedman, J.M. (2010). Antidiabetic effects of IGFBP2, a leptin-regulated gene. Cell Metab. *11*, 11–22.

Kleiner, D.E., Brunt, E.M., Van Natta, M., Behling, C., Contos, M.J., Cummings, O.W., Ferrell, L.D., Liu, Y.-C., Torbenson, M.S., Unalp-Arida, A., et al.; Nonalcoholic Steatohepatitis Clinical Research Network. (2005). Design and validation of a histological scoring system for nonalcoholic fatty liver disease. Hepatology *41*, 1313–1321.

Kusminski, C.M., Holland, W.L., Sun, K., Park, J., Spurgin, S.B., Lin, Y., Askew, G.R., Simcox, J.A., McClain, D.A., Li, C., and Scherer, P.E. (2012). MitoNEET-driven alterations in adipocyte mitochondrial activity reveal a crucial adaptive process that preserves insulin sensitivity in obesity. Nat. Med. *18*, 1539–1549.

Lundell, L. (2012). Principles and results of bariatric surgery. Dig. Dis. *30*, 173–177.

Mathurin, P., Gonzalez, F., Kerdraon, O., Leteurtre, E., Arnalsteen, L., Hollebecque, A., Louvet, A., Dharancy, S., Cocq, P., Jany, T., et al. (2006). The evolution of severe steatosis after bariatric surgery is related to insulin resistance. Gastroenterology *130*, 1617–1624.

Neph, S., Vierstra, J., Stergachis, A.B., Reynolds, A.P., Haugen, E., Vernot, B., Thurman, R.E., John, S., Sandstrom, R., Johnson, A.K., et al. (2012). An expansive human regulatory lexicon encoded in transcription factor footprints. Nature *489*, 83–90.

Pogribny, I.P., Tryndyak, V.P., Bagnyukova, T.V., Melnyk, S., Montgomery, B., Ross, S.A., Latendresse, J.R., Rusyn, I., and Beland, F.A. (2009). Hepatic epigenetic phenotype predetermines individual susceptibility to hepatic steatosis in mice fed a lipogenic methyl-deficient diet. J. Hepatol. *51*, 176–186.

R Development Core Team. (2010). R: A Language and Environment for Statistical Computing (Vienna, Austria: R Foundation for Statistical Computing).

Romeo, S., Kozlitina, J., Xing, C., Pertsemlidis, A., Cox, D., Pennacchio, L.A., Boerwinkle, E., Cohen, J.C., and Hobbs, H.H. (2008). Genetic variation in PNPLA3 confers susceptibility to nonalcoholic fatty liver disease. Nat. Genet. *40*, 1461–1465.

Sookoian, S., Rosselli, M.S., Gemma, C., Burgueño, A.L., Fernández Gianotti, T., Castaño, G.O., and Pirola, C.J. (2010). Epigenetic regulation of insulin resistance in nonalcoholic fatty liver disease: impact of liver methylation of the peroxisome proliferator-activated receptor γ coactivator 1α promoter. Hepatology *52*, 1992–2000.

Stadler, M.B., Murr, R., Burger, L., Ivanek, R., Lienert, F., Schöler, A., van Nimwegen, E., Wirbelauer, C., Oakeley, E.J., Gaidatzis, D., et al. (2011). DNA-binding factors shape the mouse methylome at distal regulatory regions. Nature *480*, 490–495.

Takahashi, Y. (2012). Essential roles of growth hormone (GH) and insulin-like growth factor-I (IGF-I) in the liver. Endocr J. *59*, 955–962.

Tran, T.T., Yamamoto, Y., Gesta, S., and Kahn, C.R. (2008). Beneficial effects of subcutaneous fat transplantation on metabolism. Cell Metab. *7*, 410–420.

Wang, Q., Jiang, L., Wang, J., Li, S., Yu, Y., You, J., Zeng, R., Gao, X., Rui, L., Li, W., and Liu, Y. (2009). Abrogation of hepatic ATP-citrate lyase protects against fatty liver and ameliorates hyperglycemia in leptin receptor-deficient mice. Hepatology *49*, 1166–1175.